

Magnetization of a dilute magnetic alloy with magnetic interactions: ZnMn[†]

F. W. Smith

Department of Physics, The City College of the City University of New York, New York, New York 10031

(Received 7 February 1974)

We have measured the magnetization M up to 50 kG at low temperatures (1.2–4.2 K) of a series of ZnMn alloys ($n = 60$ –2500 ppm Mn). For the alloys studied, the measured magnetization is dominated by impurity-impurity interactions via the indirect Ruderman-Kittel-Kasuya-Yosida (RKKY) potential $V(r) = (V_0 \cos 2k_F r)/r^3$. These interactions reduce M below the Brillouin function $B_S(H/T)$ appropriate for free spins, and also inhibit the approach to saturation of M . In the limit $n \rightarrow 0$, the measured M remains below the free-spin Brillouin function. For the $n = 60, 112,$ and 213 ppm Mn alloys and for $g\mu_B H \gg k_B T$, we find $M = g\mu_B S n [1 - H_0(n, T)/H]$, where S is the spin of the Mn impurity and $H_0(n, T) = A k_B T + B n V_0$. For these alloys we find $A/B = 0.16 \pm 0.03$ and $V_0 = (1.7 \pm 0.4) \times 10^{-36}$ erg cm³. The term $A k_B T$ in $H_0(n, T)$ may represent a single-impurity (Kondo) effect, while the term $B n V_0$ clearly represents the effects of the RKKY potential. Scaling behavior is observed for the magnetization once the concentration dependence of the impurity spin S is accounted for in the following way: $M/nS(n) = F_1(T/n, H/n)$. However, deviations from scaling of M are observed for the 2500-ppm Mn alloy where evidence has been found for additional interactions not of the RKKY type. The scaling behavior of the zero-field magnetic susceptibility is also presented.

I. INTRODUCTION

When dilute concentrations of magnetic impurities are randomly distributed in nonmagnetic metals, the interaction between the conduction electrons and the localized magnetic moments of the impurities gives rise to a variety of interesting concentration- and temperature-dependent effects which are observable experimentally in the thermal, magnetic, and transport properties of the alloy.¹ Of primary importance to this problem is the s - d interaction $-J\vec{S}\cdot\vec{\sigma}$, where J is the exchange integral, \vec{S} is the localized spin, and $\vec{\sigma}$ is the spin of the conduction electron. The s - d interaction is responsible for both single-impurity (Kondo) effects¹ and for the effects due to indirect impurity-impurity interactions via the Ruderman-Kittel-Kasuya-Yosida (RKKY) potential.² The characteristic energy for the single-impurity effects is $k_B T_K$, where T_K is the Kondo temperature, while for the impurity-impurity effects the characteristic energy is nV_0 , where n is the concentration of magnetic impurities and V_0 is the strength of the RKKY interaction $V(r) = (V_0 \cos 2k_F r)/r^3$.

Thus if $k_B T_K > nV_0$, single-impurity effects will dominate, if $k_B T_K < nV_0$, impurity-impurity interactions will dominate, and if $k_B T_K \sim nV_0$, both interactions will determine the experimental behavior. It is clearly essential to determine both T_K and V_0 for a given alloy system. The primary goals of this investigation are to further develop our ability to separate single-impurity effects from impurity-impurity effects within a given alloy system, and subsequently to study the interactions

[single-impurity-conduction-electron (Kondo) or impurity-impurity] themselves.

At very low concentrations n when the magnetic impurities act independently of one another, theory predicts that experimentally observed quantities, such as magnetization and zero-field magnetic susceptibility, will be universal functions of T/T_K . Thus, in the single-impurity limit we can write $M/n = f_1(T/T_K)$ and $\chi/n = f_2(T/T_K)$. At higher concentrations n when the RKKY interactions between impurities dominate the behavior of the alloy, theory predicts that universal scaling laws will be obeyed,^{3,4} with a scaling parameter which in this case is n (as opposed to T_K), with the result that $M/n = F_1(T/n, H/n)$ and $\chi = F_2(T/n)$. For free spins it should be pointed out that a Brillouin function describes the magnetization: $M/n = B_S(H/T)$. A modified Brillouin function has also been used to fit magnetization data, namely, $M/n = B_S[H/(T+\Theta)]$, where Θ is a constant to be determined empirically.⁵

At high T (such that $k_B T \gg nV_0$), Larkin *et al.*⁶ have used a virial expansion of the free energy in a power series of the concentration of impurities n to investigate the effect of the RKKY potential on the thermodynamic functions of dilute magnetic alloys. They predict for $k_B T \gg nV_0$ and for $H \rightarrow 0$ that

$$\chi = n g^2 \mu_B^2 S(S+1)/3(k_B T + \Theta),$$

where $\Theta = C_S n V_0$ and C_S is a constant of order unity. In addition, in a high magnetic field, such that $g\mu_B H$ is much greater than both $k_B T$ and nV_0 , they

predict for the approach to saturation of the magnetization

$$M = g\mu_B S n [1 - 2(2S + 1)nV_0/3g\mu_B H]. \quad (1)$$

It should be noted that for $g\mu_B H \gg k_B T$, Eq. (1) is expected to correctly describe M for all T .

At very low temperatures or very high concentrations ($k_B T \ll nV_0$), a dilute magnetic alloy enters the spin-glass regime,⁷ where the impurity spins are strongly correlated with each other but without long-range magnetic order present. Klein⁸ has predicted the limiting low- T behavior of a dilute magnetic alloy by considering a random molecular field H which has a probability distribution function $P(H) = \Delta/\pi(\Delta^2 + H^2)$, where Δ is the width of $P(H)$. As $T \rightarrow 0$ for the susceptibility it is predicted that $\chi(H \rightarrow 0) = 2n\mu_B/\pi\Delta$ and for the magnetization that

$$M = (2n\mu_B/\pi) \tan^{-1}(H/\Delta), \quad (2)$$

where μ_B is the magnetic moment of the spin $S = \frac{1}{2}$ impurity.^{8,9} Thus for $H \gg \Delta$, Eq. (2) predicts for the approach to saturation $M = n\mu_B [1 - (2\Delta/\pi H)]$. In this limit, Eqs. (1) and (2) are in agreement, with Δ proportional to nV_0 .

We have been successful in verifying over what range of n and T impurity-impurity interactions dominate the behavior of a series of ZnMn alloys. Specific-heat measurements^{10,11} yielding $\Delta C/n$ proportional to n/T for $T/n > 6 \times 10^{-3}$ K/ppm and $n > 200$ ppm, in agreement with theory,⁶ have enabled us to determine $S = \frac{3}{2}$ and $V_0 = 0.9 \times 10^{-36}$ erg cm³ for ZnMn. We have proposed an expression for $\Delta C(n, T)$ which has proven to be in excellent agreement with both theory and experiment over a wide range of n and T , namely, $\Delta C = AT/(1 + BT^2/n^2)$.^{10,11} Magnetic-susceptibility measurements¹² have verified that Θ is proportional to nV_0 for $n > 100$ ppm Mn, in agreement with the prediction of Larkin.⁶ These measurements of $\chi(H \rightarrow 0)$ have also demonstrated for the first time in a dilute magnetic-alloy system that there is a minimum in the Curie-Weiss temperature Θ and in the effective magnetic moment μ_{eff} as n increases. We have determined

$$V_0 = (2.25 \pm 0.2) \times 10^{-36} \text{ erg cm}^3$$

from $\Theta(n)$.¹²

To further investigate the competition between single-impurity (Kondo) and impurity-impurity interactions in ZnMn, we have measured the magnetization M in external magnetic fields up to 50 kG at low temperatures (1.2–4.2 K) of a series of ZnMn alloys (60–2500 ppm Mn). The single-impurity (Kondo) and impurity-impurity interactions will both inhibit the ability of the impurity spins to align themselves in an external magnetic field. Deviations of the impurity magnetization

M from the Brillouin function $B_S(H/T)$ expected for free spins should thus be observed. By measuring M over a wide range of n and H , and comparing the observed behavior with theoretical predictions, we have determined over what range of n impurity-impurity interactions dominate the observed behavior of M for the temperature range studied.

II. EXPERIMENTAL

Magnetization measurements from 0 to 50 kG and from 1.2 to 4.2 K have been made on a series of ZnMn alloys (60-, 112-, 213-, 530-, 1065-, 2500-ppm Mn). In addition, measurements of M above 4.2 K were made for 60-, 1065-, and 2500-ppm alloys. Details of sample preparation have been given earlier.^{10,11} The concentrations n of Mn impurities were determined from measured resistance ratios

$$\rho = R(4.2)/[R(273) - R(4.2)]$$

and $\rho/n = 2.82/\text{at.}\% \text{ Mn}$. It has been predicted that ρ/n will be a decreasing function of n , due to magnetic interactions between the impurities.⁶ This correction, which is on the order of 10% for $n = 200$ ppm Mn, does not affect the conclusions of this work and has been neglected.

The magnetization has been measured by the Faraday method using a Cahn RH Electrobalance (resolution 2 μg) and a Westinghouse superconducting solenoid (0–50 kG). Details of the experimental apparatus appear elsewhere.¹³ The polycrystalline magnetization samples were roughly in the form of cubes with dimensions typically of 3–5 mm and masses of 0.2–1 g. These samples were cut from the cylindrical samples (1.3 cm in diameter by 5 cm long) used previously in specific-heat measurements.^{10,11} The 1065- and 2500-ppm-Mn alloys were cut from opposite ends of the nominally 1200-ppm-Mn sample, in which concentration gradients had previously been detected.^{10,11} Thermometry was provided from 1.2 up to 20 K by a calibrated Allen Bradley carbon resistor, while from 20 to 77 K a platinum resistance thermometer was used. These thermometers were calibrated against the susceptibility of chrome potassium alum.

Magnetization curves for these alloys were obtained by plotting the unbalance of the Cahn RH electrobalance as a function of applied magnetic field on an x - y recorder. For the 60- and 112-ppm-Mn samples the magnetization M due to the Mn impurities was corrected for de Haas-van Alphen oscillations due to the presence of large single crystals in the samples. For all the samples, the magnetization was corrected for the con-

tribution from the diamagnetic susceptibility of pure Zn, which was measured to be -0.145×10^{-6} emu/g at 1.2 and 4.2 K.¹²

III. RESULTS AND DISCUSSION

In Figs. 1(a) and 1(b) the impurity magnetization $M/g\mu_B Sn$ is plotted as a function of H at $T=1.26$ and 4.25 K, respectively, for the six concentrations studied here (60-, 112-, 213-, 530-, 1065-, and 2500-ppm Mn). Also shown is a Brillouin function of spin $S = \frac{3}{2}$ for the appropriate temperature. In Table I we list the concentrations n and effective spins S for these alloys. These concentrations and the effective spins determined from the Curie constants, along with $g=2$, have been used to normalize the magnetization M in Figs. 1, 2, and 3.

It is apparent that the impurity magnetization M in Figs. 1(a) and 1(b) does not follow the Brillouin function expected for free spins, which reaches saturation much more rapidly as a function of applied field. Nor is M solely the result of a single-impurity (Kondo) effect as $M/g\mu_B Sn$ is a function of both T and n . Instead we find that, at a

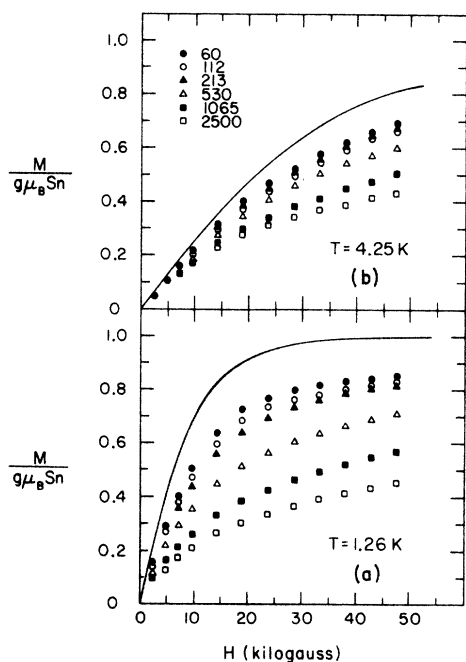


FIG. 1. Impurity magnetization as a function of applied magnetic field H at (a) $T = 1.26$ K and (b) 4.25 K for the six alloys studied here. The magnetization M has been normalized to $g\mu_B Sn$ where $g = 2$, S is the effective spin obtained from the measured Curie constant (see Table I), and n is the measured concentration. Also shown as the solid curve is the free-spin Brillouin function $B_{3/2}(H/T)$ for $S = \frac{3}{2}$ at the appropriate temperature. For clarity, not all of the data points at low magnetic fields have been plotted.

given H and T , the magnetization per spin decreases as n increases. This behavior is similar to that previously observed in CuMn,¹⁴ and is a characteristic feature of magnetic interactions which arise from the RKKY potential.^{6,8}

In Fig. 2, $M/g\mu_B Sn$ is plotted as a function of n for $T=1.26$ and 4.25 K in a field of 47.45 kG. For $n < 1000$ ppm Mn, the magnetization per spin decreases linearly with n , in agreement with the virial expansion theory of Larkin.⁶ The measured value of $M/g\mu_B Sn$ for the 2500-ppm-Mn alloy falls above the extrapolated linear decrease, indicating either the presence of a positive n^2 term in the virial expansion of $M/g\mu_B Sn$ or a contribution from additional interactions at higher concentrations not of the RKKY type. Evidence for such additional interactions has been previously reported for this 2500-ppm-Mn alloy from magnetic-susceptibility measurements.¹²

It should be noted that the linear extrapolation of $M/g\mu_B Sn$ to $n=0$ from Fig. 2 falls below the Brillouin function for $S = \frac{3}{2}$ evaluated for this H and T . Thus the single-impurity ($n \rightarrow 0$) limit does not correspond to the free-spin prediction. Rather, the impurity magnetization per spin in this limit may be reduced below that of a free spin as a result of single-impurity (Kondo) effects.¹⁵ In dilute AgMn it has been recently observed that the measured magnetization, which exhibits impurity-impurity ordering, approaches a Brillouin function at sufficiently low impurity concentrations.¹⁶ It should be noted that AgMn has a Kondo temperature at least an order of magnitude less than that of ZnMn.¹⁷

To confirm that the magnetic interactions determining the behavior of M are RKKY, in Figs. 3(a) and 3(b) we plot M/nS as a function of H/n for four alloys at fixed $T/n = (5.95 \pm 0.05) \times 10^{-3}$ K/ppm. For RKKY interactions it is predicted that

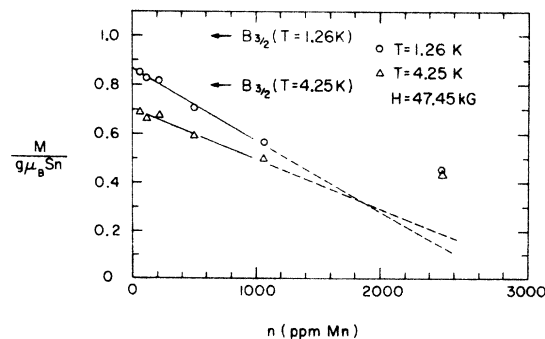


FIG. 2. Impurity magnetization M , normalized to $g\mu_B Sn$ (see text), as a function of concentration n in a magnetic field of 47.45 kG and at $T = 1.26$ and 4.25 K. Also indicated is the free-spin Brillouin function $B_{3/2}(H/T)$ for $S = \frac{3}{2}$ at the appropriate H and T .

TABLE I. Properties of ZnMn alloys studied.

n^a (ppm Mn)	S^b	S^c	nV_0/k_B (K) ^d	$\frac{2(2S+1)nV_0}{3g\mu_B}$ (kG) ^e
60 ± 1	1.32 ± 0.05	1.29 ± 0.04	0.058	1.05
112 ± 1	1.30 ± 0.05	1.21 ± 0.02	0.109	1.94
213 ± 10	1.36 ± 0.03	1.32 ± 0.02	0.207	3.82
530 ± 30	1.45 ± 0.04	...	0.515	9.96
1065 ± 50	1.60 ± 0.04	...	1.03	21.6
2500 ± 100	1.67 ± 0.06	...	2.43	52.3

^a Concentration n of Mn impurities (in ppm) as determined from measured resistance ratios ρ and $\rho/n = 2.82/\text{at. \% Mn}$.

^b Effective spin per Mn impurity as determined from measured Curie constant; see Ref. 12.

^c Effective spin per Mn impurity as determined from saturation magnetization $g\mu_B S n$ with $g=2$, from this work. We did not approach saturation for the three higher concentration alloys in magnetic fields up to 50 kG because of the stronger magnetic interactions present in these alloys.

^d Effective "interaction temperatures" for these alloys. We use for ZnMn $V_0 = 2 \times 10^{-36}$ erg cm³ and 1 ppm Mn = 0.67×10^{17} Mn impurities per cm³.

^e Magnitude of correction term (in kG) in Eq. (1). We have used for ZnMn $V_0 = 2 \times 10^{-36}$ erg cm³, 1 ppm Mn = 0.67×10^{17} Mn impurities per cm³, $g=2$, and the spin S (from the second column of this table) determined from the measured Curie constant.

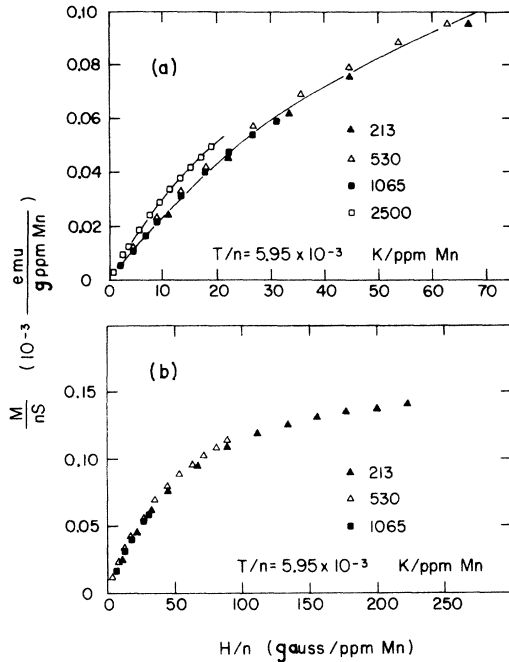


FIG. 3. Impurity magnetization M , normalized to nS (see text), as a function of H/n at the "reduced temperature" $T/n = (5.95 \pm 0.05) \times 10^{-3}$ K/ppm Mn. Here S is the effective spin obtained from the Curie constant. For $n = 213, 530, 1065, 2500$ ppm Mn, the corresponding temperatures are $T = 1.26, 3.16, 6.33, 15$ K and the corresponding spins are $S = 1.36, 1.45, 1.60, 1.67$ (from Table I). For clarity, overlapping data points have been omitted.

$M/n = F_1(T/n, H/n)$, so that our results as plotted in Fig. 3 will fall on a universal curve for those alloys in which RKKY interactions dominate. We observe scaling for the $n = 213, 530,$ and 1065 ppm Mn alloys when we account for the concentration-dependence of S by plotting M/nS instead of M/n . It should be noted that the theories which predict scaling do not include a spin S , or effective magnetic moment $\mu_{\text{eff}} = g\mu_B[S(S+1)]^{1/2}$, which depends on n .^{3,4}

From Fig. 3(b) it can be seen that M/nS for the 2500-ppm-Mn alloy does not scale with the other alloys even after the dependence of S on n has been accounted for. Instead, there appears to be an additional contribution to M/nS for this alloy, which is consistent with our discussion of Fig. 2 and the results of magnetic-susceptibility measurements.¹² Similar scaling behavior with deviations at increasing concentrations has been previously observed in CuMn.⁴

Scaling for the magnetic susceptibility $\chi(H=0)$ is displayed in Fig. 4 where, to account for the dependence of μ_{eff}^2 on n , $\chi/S(S+1)$ is plotted as a function of T/n . Deviations from scaling are observed both at low concentrations ($n = 21$ ppm Mn) where single-impurity (Kondo) effects dominate, and at high concentrations ($n = 2500$ ppm Mn) where additional interactions are present. However, there is a region of almost two decades in T/n , $2 \times 10^{-3} - 2 \times 10^{-1}$ K/ppm, for which scaling is reasonably well obeyed for the intermediate concentration alloys, 60–1065-ppm Mn.

Since the measured magnetization for the 60-, 112-, and 213-ppm-Mn alloys as shown in Fig. 1 indicates an approach to saturation in these magnetic fields, we can compare our results with the prediction of Larkin *et al.*⁶ for the magnetization, valid in the limit $g\mu_B H \gg k_B T$, given in Eq. (1). To test Larkin's prediction, expected to apply to alloys for which the second term in the brackets is a small correction, we show in Fig. 5 our results for M for these three alloys plotted versus $1/H$ for several temperatures. It is apparent that the functional form of Eq. (1) correctly describes the approach to saturation of these three alloys. In the limit $1/H \rightarrow 0$ ($H \rightarrow \infty$), the magnetization curves shown in Fig. 5 for a given alloy approach a saturation limit which is essentially independent¹⁸ of T and only slightly lower than the value $M_{\text{sat}} = g\mu_B S n$ calculated using $g=2$, the spin S obtained from the Curie constant (Table I), and the measured concentration n . Using the measured M_{sat} , we calculate the effective spin $S = M_{\text{sat}}/2\mu_B n$, also listed in Table I. The agreement between these two values of the spin S for each of these three alloys is reasonably good.

Equation (1) predicts that the slope of M versus $1/H$ as plotted in Fig. 5 should be independent of T . This is not the case for these three alloys as we find the slope increasing as T increases. We find that the measured magnetization can be represented by the following expression:

$$M = g\mu_B S n [1 - H_0(n, T)/H], \quad (3)$$

where $H_0(n, T) = Ak_B T + BnV_0$. By comparison with Eq. (1) we make the following identification:

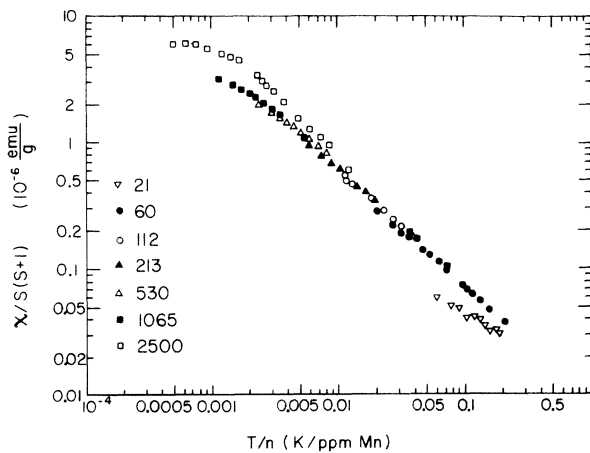


FIG. 4. Magnetic susceptibility $\chi(H \rightarrow 0)$ divided by $S(S+1)$ for seven ZnMn alloys (21, 60, 112, 213, 530, 1065, and 2500 ppm Mn) as a function of "reduced temperature" T/n . For these alloys, $S(S+1)$ has been obtained from the measured Curie constant and $g=2$. For clarity, overlapping data points have been omitted.

$B = 2(2S+1)/3g\mu_B$. In Fig. 6 we plot $H_0(n, T)/n = Ak_B T/n + BV_0$ as a function of T/n for these three alloys. The straight line drawn through the data points has an intercept at $T/n=0$ equal to BV_0 and a slope equal to Ak_B . Note that the data for the three alloys will fall on a single straight line if the coefficients A and B are independent of n and T . Since B is proportional to $(2S+1)$, there is a weak dependence ($\sim 5\%$, see Table I) on n for this quantity, which we will ignore.

From the intercept of the straight line drawn in Fig. 6 we find $BV_0 = (2.2 \pm 0.5) \times 10^{-16}$ G cm³ and hence $V_0 = (1.7 \pm 0.4) \times 10^{-36}$ erg cm³, using $g=2$ and an average spin $S = 1.33$ to determine $B = 2(2S+1)/3g\mu_B$. From the slope we find $Ak_B = (2.9 \pm 0.45) \times 10^3$ G/K. For the ratio of the coefficients appearing in $H_0(n, T) = Ak_B T + BnV_0$, we find $A/B = 0.16 \pm 0.03$. It should be pointed out that a better fit to the data in Fig. 6 could be obtained with a separate straight line for each alloy. However, we do not feel that this procedure would be meaningful in light of the scatter in the data. Instead we have chosen to determine a single intercept BV_0 and a single slope Ak_B whose stated uncertainties include the variations observed for the three alloys.

In order to be able to follow the procedure described above, for the 530-, 1065-, and 2500-

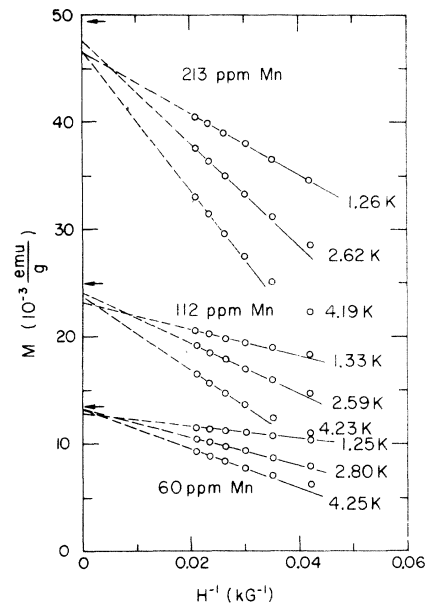


FIG. 5. Impurity magnetization M for the $n = 60$, 112, and 213 ppm Mn alloys as a function of the inverse of the magnetic field $1/H$ for several temperatures. The arrows on the left hand vertical axis indicate the values of $M_{\text{sat}} = g\mu_B S n$ calculated using $g=2$, the effective spins S from the measured Curie constant (see Table I), and the measured concentrations n .

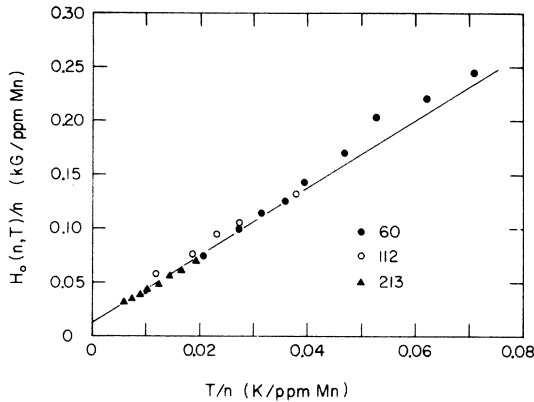


FIG. 6. $H_0(n, T)/n$ as a function of "reduced temperature" T/n for the 60-, 112-, and 213-ppm-Mn alloys. The straight line indicates our fit to the equation $H_0(n, T)/n = Ak_B T/n + BV_0$ [see Eq. (3) for the definition of $H_0(n, T)$].

ppm-Mn alloys it would be necessary to extend our measurements of magnetization M either to higher magnetic fields H or lower temperatures T , as we have not approached saturation for these alloys. As can be seen from Table I the correction term in Eq. (1) is not small compared to 50 kG for these alloys.

The presence of the term $Ak_B T$ in $H_0(n, T)$ of Eq. (3) remains to be explained. To identify our empirical parameter $H_0(n, T)$ with a concentration- and temperature-dependent width $\Delta(n, T)$ of $P(H)$ to be used in Klein's Eq. (2) does not appear correct since $\Delta(n, T)$ is predicted theoretically⁸ to be a decreasing function of T , whereas $H_0(n, T) = Ak_B T + BnV_0$ is an increasing function of T . Also, it is extremely difficult to see how $\Delta(n, T)$ could remain finite and equal to $Ak_B T$ in the limit $n \rightarrow 0$. The $-Ak_B T/H$ term in M cannot be attributed to free-spin behavior in the limit $n \rightarrow 0$ since the Brillouin function $B_S(H/T)$ approaches saturation for $g\mu_B H/k_B T \gg 1$ much faster than $1 - Ak_B T/H$. The possibility remains that this term represents a single-impurity (Kondo) effect.

IV. CONCLUSIONS

It has been shown that the measured magnetization of these ZnMn alloys is dominated by impurity-

impurity interactions via the indirect RKKY potential. Scaling behavior is observed for the magnetization per spin M/nS with deviations occurring at high concentrations, $n = 2500$ ppm Mn, where an additional contribution to M/nS is found. The single-impurity ($n \rightarrow 0$) limit of the magnetization M falls below the Brillouin function expected for free spins, which may indicate the presence of the Kondo effect.

For the three most dilute alloys, $n = 60$, 112, and 213 ppm Mn, we have compared the measured magnetization M to the prediction of Larkin, Eq. (1). The $1/H$ approach of M to saturation has been verified, but with a slope $H_0(n, T)$ which is both concentration and temperature dependent, in contrast to the theory. From the slope in the limit $T/n \rightarrow 0$ we have determined $V_0 = (1.7 \pm 0.4) \times 10^{-36}$ erg cm³, in good agreement with results previously obtained from magnetic-susceptibility¹² ($V_0 = 2.25 \times 10^{-36}$ erg cm³) and specific-heat^{10,11} ($V_0 = 0.9 \times 10^{-36}$ erg cm³) measurements on these alloys. From M in the limit $1/H \rightarrow 0$, we have obtained values for the spin S in good agreement with results obtained from magnetic-susceptibility measurements.¹²

Although RKKY interactions dominate the observed behavior of these ZnMn alloys over a wide range of concentrations, it is clear that further theoretical work on the properties of dilute magnetic alloy systems such as ZnMn needs to take into account both single-impurity (Kondo) effects and impurity-impurity (RKKY) interactions at low concentrations n and impurity-impurity interactions more complicated than RKKY at higher concentrations. Crystal-field splitting in ZnMn will also be a competing effect and is expected to be important at low temperatures (less than 1 K).¹⁹

ACKNOWLEDGMENTS

We wish to acknowledge useful discussions with J. B. Haddad, M. P. Sarachik, M. W. Klein, and F. T. Hedgcock. Thanks also to J. C. Liu and S. Rochlitz for assistance with some of these measurements.

[†]Research supported by the National Science Foundation under Grant No. GH-34672 and by CUNY FRAP Grant No. 10646.

¹For reviews of both the theoretical and experimental sides of the Kondo effect, see, *Magnetism*, edited by H. Suhl (Academic, New York, 1973), Vol. 5.

²M. A. Ruderman and C. Kittel, *Phys. Rev.* **96**, 99 (1954); K. Yosida, *ibid.* **106**, 893 (1957); T. Kasuya,

Prog. Theor. Phys. **16**, 45 (1956).

³A. Blandin, thesis (Paris University, 1961) (unpublished); A. Blandin and J. Friedel, *J. Phys. Radium* **20**, 160 (1959).

⁴J. Souletie and R. Tournier, *J. Low Temp. Phys.* **1**, 95 (1969).

⁵See A. Narath, Ref. 1, p. 161.

⁶A. I. Larkin and D. E. Khmel'nitskii, *Zh. Eksp. Teor.*

Fiz. 58, 1789 (1970) [Sov. Phys.-JETP 31, 958 (1970)]; A. I. Larkin, V. I. Mel'nikov, and D. E. Khmel'nitskii, Zh. Eksp. Teor. Fiz. 60, 846 (1971) [Sov. Phys.-JETP 33, 458 (1971)].

⁷For a good review of the theory of spin glasses see

P. W. Anderson, in *Proceedings of the International Symposium on Amorphous Magnetism*, edited by H. O. Hooper and A. M. DeGraff (Plenum, New York, 1973), p. 1.

⁸M. W. Klein and R. Brout, Phys. Rev. 132, 2412 (1963); M. W. Klein, *ibid.* 136, A1156 (1964); 173, 552 (1968).

⁹A. A. Abrikosov, Usp. Phys. Nauk. 97, 403 (1969) [Sov. Phys.-Usp. 12, 168 (1969)].

¹⁰F. W. Smith, Solid State Commun. 13, 1267 (1973).

¹¹F. W. Smith, Phys. Rev. B 9, 942 (1974).

¹²F. W. Smith, in Proceedings of the 1973 Conference on Magnetism and Magnetic Materials, edited by C. D. Graham, Jr. and J. J. Rhyne (AIP, New York, 1974),

p. 975.

¹³J. B. Haddad, thesis (City College of the City University of New York, 1974) (unpublished).

¹⁴See J. M. Franz and D. J. Sellmyer, Phys. Rev. B 8, 2083 (1973), and references therein.

¹⁵P. E. Bloomfield, R. Hecht, and P. R. Sievert, Phys. Rev. B 2, 3714 (1970).

¹⁶J. C. Doran and O. G. Symko, in Ref. 12, p. 980.

¹⁷J. Flouquet, Phys. Rev. Lett. 25, 288 (1970).

¹⁸ M_{sat} decreases slightly, $\sim 3\%$, as T is lowered from 4.2 to 1.2 K for the 112- and 213-ppm-Mn alloys. For the 60-ppm-Mn alloy, the decrease is about 9%. However, the values of M measured for this alloy are not as accurate as for the other alloys due to the presence of the de Haas-van Alphen effect.

¹⁹P. L. Li, F. T. Hedgcock, W. B. Muir, and J. O. Ström-Olsen, Phys. Rev. Lett. 31, 29 (1973).